

Supplementary Material

Neuroprotective actions of a fatty acid nitroalkene in Parkinson's disease.

Roberto Di Maio^{a,b*}, Matthew T. Keeney^{a,b,c}, Veronika Cechova^c, Amanda Mortimer^{a,b}, Ahssan Sekandari^c, Pascal Rowart^c, J. Timothy Greenamyre^{a,b}, Bruce A. Freeman^c, Marco Fazzari^{c*}

^a Pittsburgh Institute for Neurodegenerative Diseases, ^b Department of Neurology, University of Pittsburgh, Pittsburgh, PA, 15213, U.S.A. ^c Department of Pharmacology and Chemical Biology, University of Pittsburgh, 200 Lothrop Street, Pittsburgh, PA, 15261, U.S.A.

*Corresponding Authors:

R. Di Maio: rod16@pitt.edu

M. Fazzari: maf167@pitt.edu

Supplementary Table 1. Antibodies used in this study.

Supplementary Figure 1. Cytotoxicity of 10-NO₂-OA in N27-A dopaminergic cells.

Supplementary Figure 2. 10-NO₂-OA prevents rotenone-induced NOX2 and LRRK2 activation and oxidative stress in vitro.

Supplementary Figure 3. 10-NO₂-OA activates Nrf2-dependent gene expression in rotenone treated N27-A dopaminergic cells.

Supplementary Figure 4. Analysis of free 10-NO₂-OA and its inactive metabolite in rat brain (cohort 2).

Supplementary Figure 5. 10-NO₂-OA inhibited lipid peroxidation (4-HNE) in the subacute PD model of rotenone.

Supplementary Figure 6. 10-NO₂-OA inhibited NOX2 activation in SNpc of rat rotenone model.

Supplementary Figure 7. 10-NO₂-OA prevented rotenone-induced LRRK2 activation in SNpc.

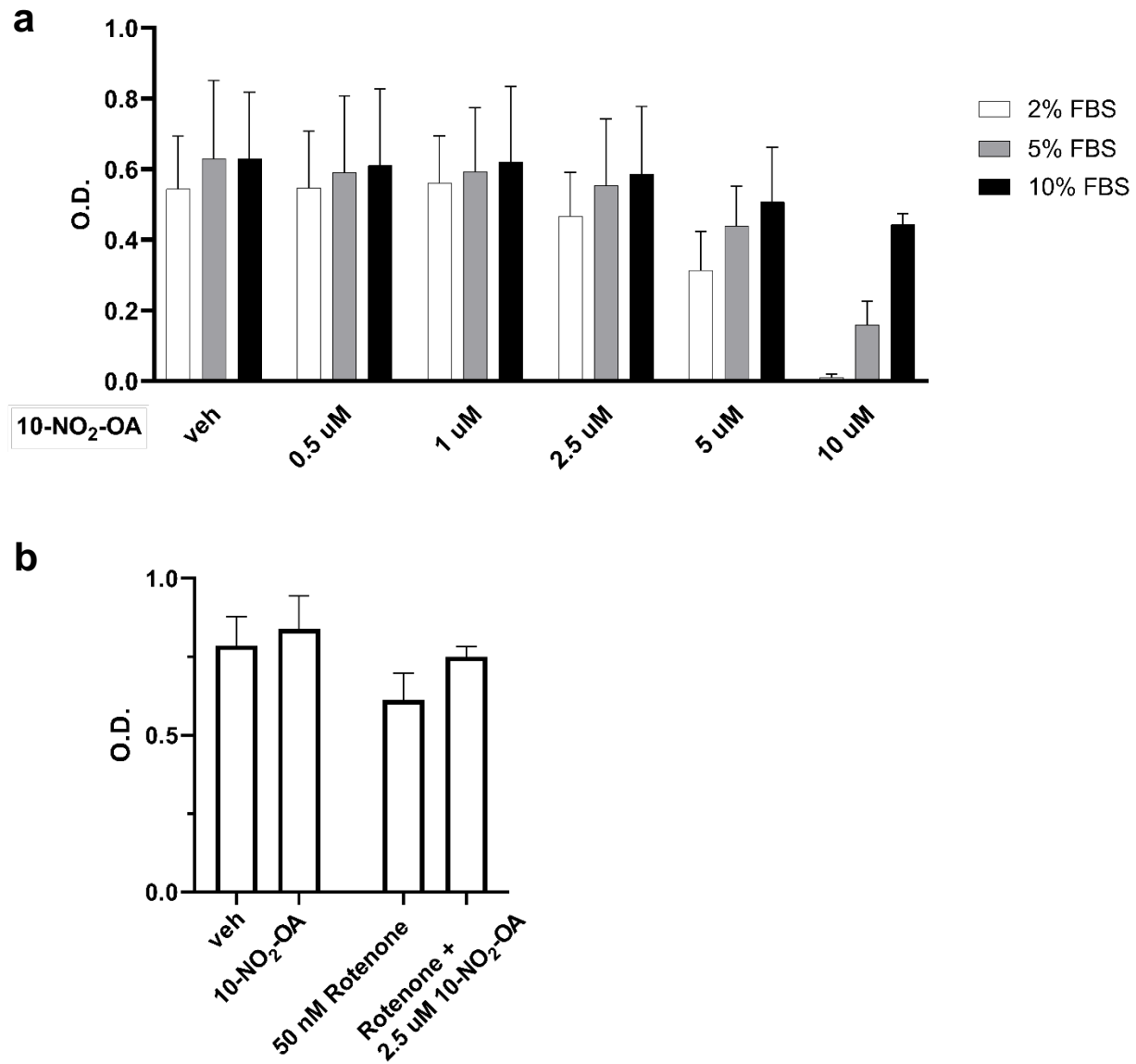
Supplementary Figure 8. Validation of PL assays for LRRK2 and NOX2 by antibody depletion.

Supplementary Figure 9. 10-NO₂-OA inhibits α -synuclein-mediated mitochondrial import impairment in the subacute PD model of rotenone.

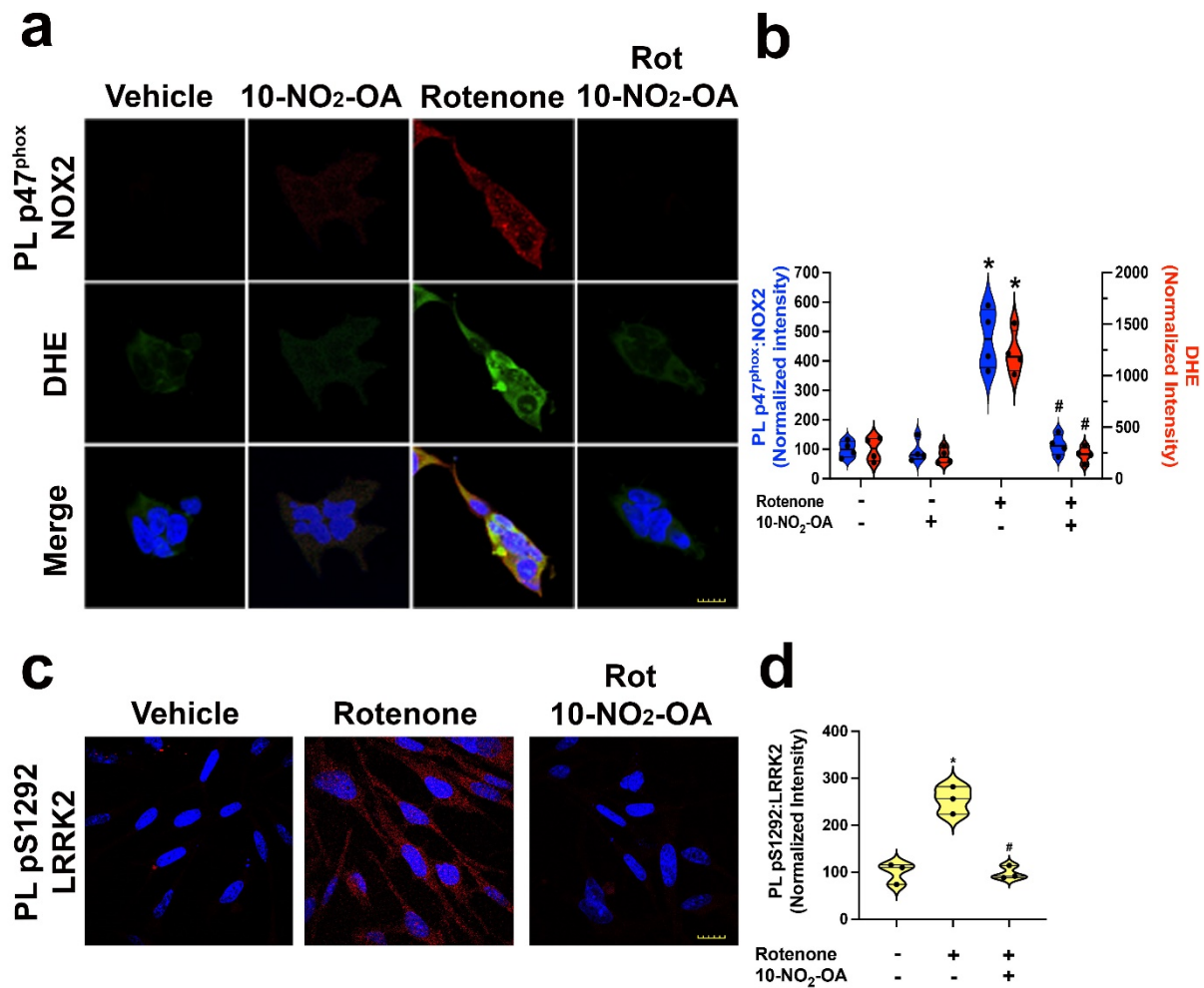
Supplementary Figure 10. Analysis of rotenone in whole rat brain (cohort 2).

Host	Antibody	Catalog #	Vendor	Dilution	Use
Mouse	NOX2/gp91 ^{phox}	ab80897	Abcam	1:1000 (ICC) 1:500 (IHC)	PLA NOX2 activity
Rabbit	NCF1[FPR13131-25] (p47 ^{phox})	ab181090	Abcam	1:1000 (ICC) 1:500 (IHC)	PLA NOX2 activity
Mouse	α -synuclein	610787	BD Transduction	1:1000 (ICC) 1:500 (IHC)	PLA 4-HNE- α -syn PLA α -syn-TOM20
Rabbit	4-hydroxynonenal	ab46545	Abcam	1:1000 (ICC) 1:500 (IHC)	PLA 4-HNE- α -syn 4-HNE IHC
Rabbit	TOM20	ab186735	Abcam	1:500 (IHC)	PLA α -syn-TOM20
Rabbit	LRRK2 (pS1292)	ab203181	Abcam	1:1000 (ICC) 1:500 (IHC)	PLA LRRK2 activity
Mouse	LRRK2 (N241A)	75-253	UC Davis	1:1000 (ICC) 1:500 (IHC)	PLA LRRK2 activity
Sheep	Tyrosine Hydroxylase	AB1542	Millipore	1:2000 (IHC)	DA neurons marker
Rabbit	Iba1	019-19741	Wako	1:500 (IHC)	Microglial marker
Mouse	Heme Oxygenase-1 (HO-1)	MA1-112	Thermo Fisher Scientific	1:250 (IHC)	HO-1 IHC
Rabbit	Nrf2	Sc-722	Santa Cruz	1:500 (IHC)	Nrf2 IHC

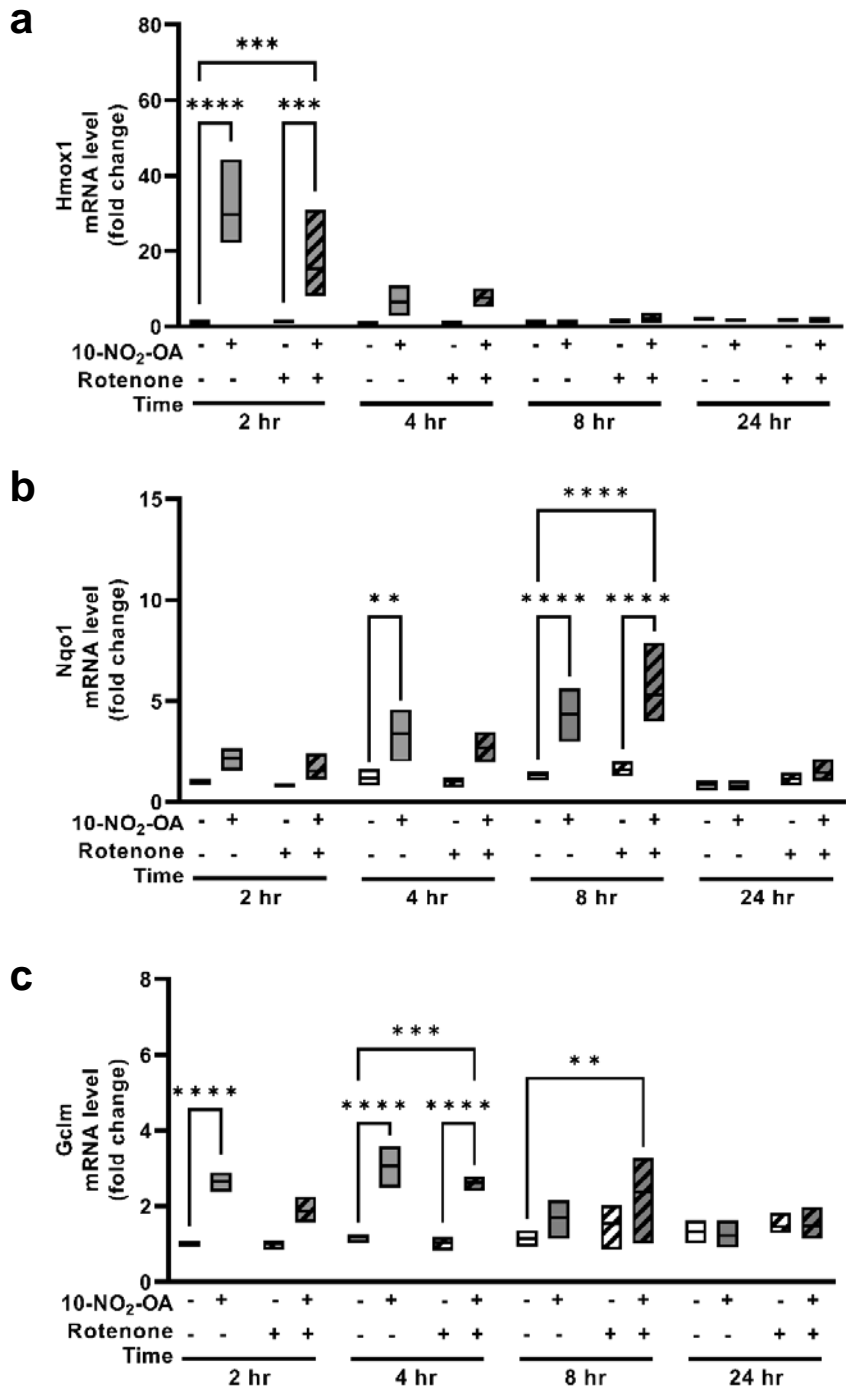
Supplementary Table 1. Antibodies used in this study.



Supplementary Figure 1. Cytotoxicity of 10-NO₂-OA in N27-A dopaminergic cells. Cell viability was assessed by MTT assay and recorded by optical density (O.D.). N27A dopaminergic cells were exposed for 24 hours to: (a) 2-5-10% FBS, Vehicle and increasing concentrations of 10-NO₂-OA (0.5 μM-10 μM). (b) Vehicle, Rotenone (50 nM) and Rotenone (50 nM) + 10-NO₂-OA (2.5 μM) in 2% FBS. All data represents the mean ± SD of at least three independent experiments with n=3.

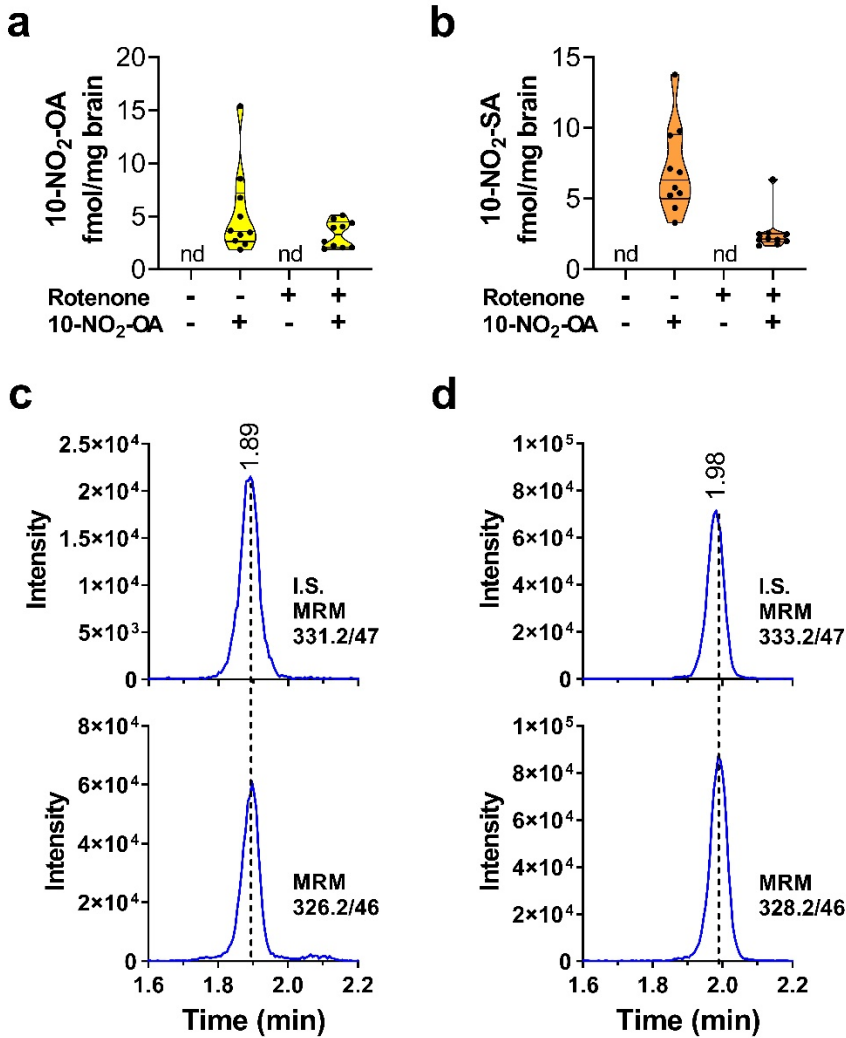


Supplementary Figure 2. 10-NO₂-OA prevents rotenone-induced NOX2 and LRRK2 activation and oxidative stress *in vitro*. N27A dopaminergic cells were exposed for 24 hours to Vehicle, Rotenone (50 nM) and Rotenone (50 nM) + 10-NO₂-OA (2.5 μM). (a) Rotenone elicited an increase in NOX2 activation as detected PL p47^{phox}:NOX2 (red). This was accompanied by an increase in cytoplasmic superoxide measured by DHE (green). Both NOX2 activation and DHE were prevented by co-treatment with 10-NO₂-OA (Scale bar: 5μm). (b) Quantitative analysis of PLA-related fluorescence intensity. (c) Co-treatment with 10-NO₂-OA prevented rotenone mediated LRRK2 activation (PL pS1292:LRRK2, red - Scale bar: 30μm). (d) Quantitative analysis of PLA-related fluorescence intensity. Each symbol represents average of normalized signal (with Vehicle set at 100%) from a single independent experiment. Statistical testing by ANOVA with post hoc Bonferroni correction (*, p<0.0001 compared to Vehicle, #, p<0.0001 compared to Rotenone).

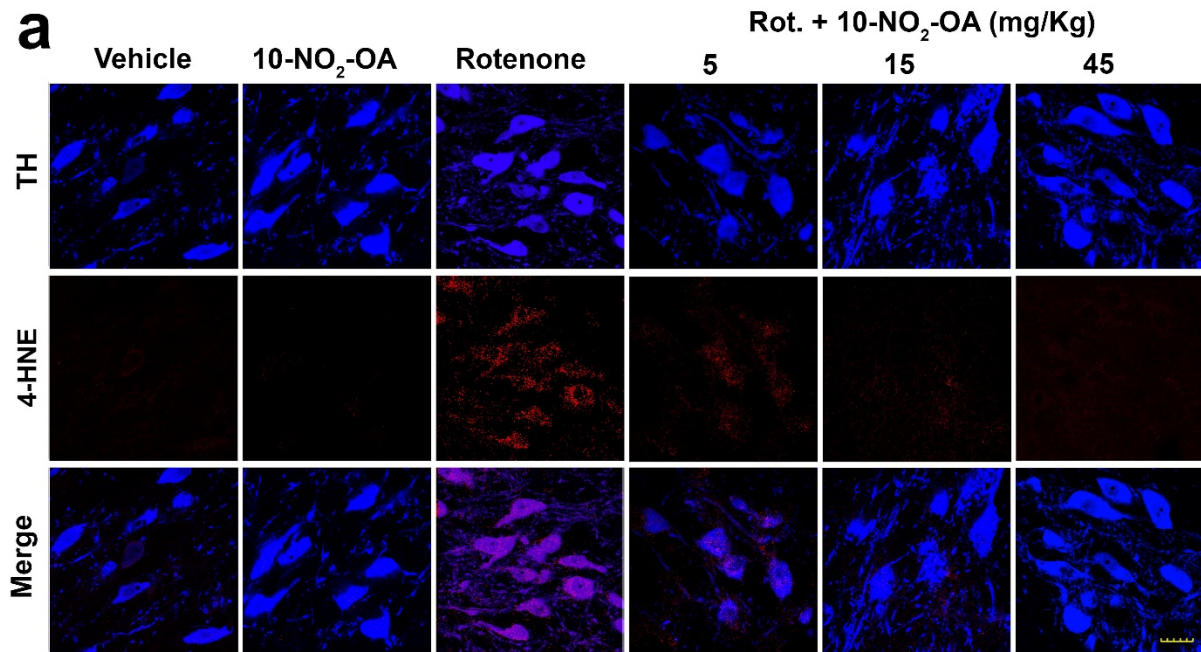


Supplementary Figure 3. 10-NO₂-OA activates Nrf2-dependent gene expression in rotenone treated N27-A dopaminergic cells. Relative mRNA levels of the following Nrf2 target genes: (a) heme oxygenase-1 (Hmx1, HO-1), (b) NAD(P)H dehydrogenase quinone-1 (Nqo-1), and (c) glutamate–cysteine ligase modifier subunit (Gclm), after treatment with 10-NO₂-OA (2.5 μM) and Rotenone (50 nM) for 2, 4, 8 and 24 hours in N27-A rat dopaminergic neural cell line. Values represent the range (minimum-maximum)

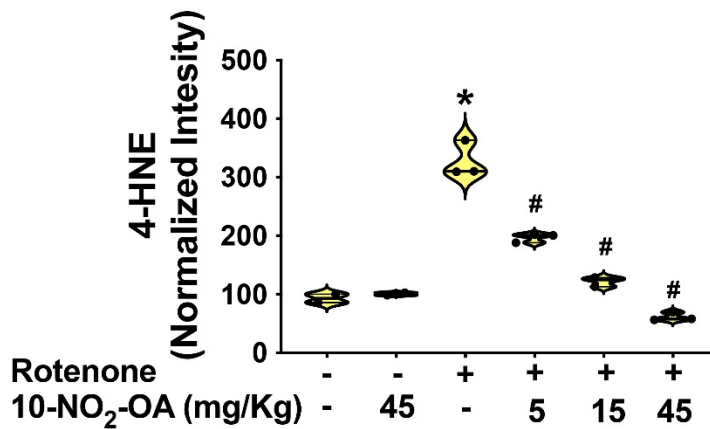
and mean of 4 independent experiments $n=1$ with statistical significance performed by two-way ANOVA with post hoc Bonferroni correction indicated by **** $p \leq 0.0001$, *** $p \leq 0.001$, and ** $p \leq 0.01$.



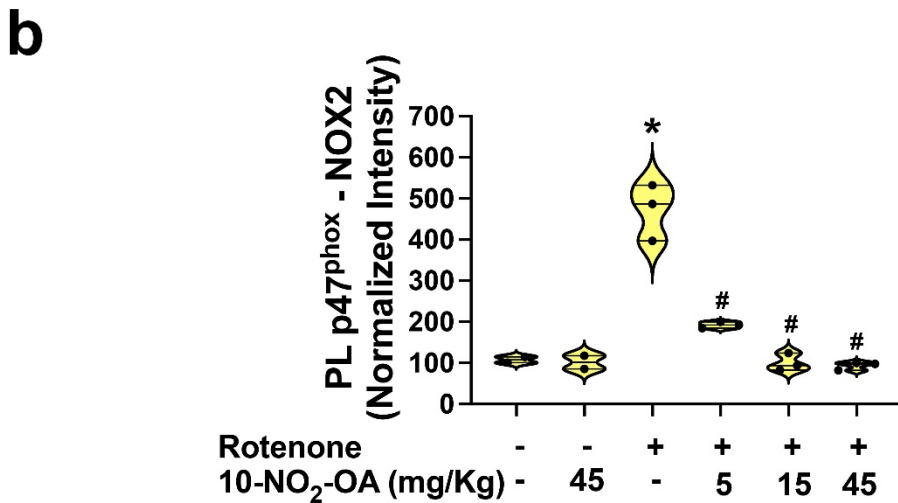
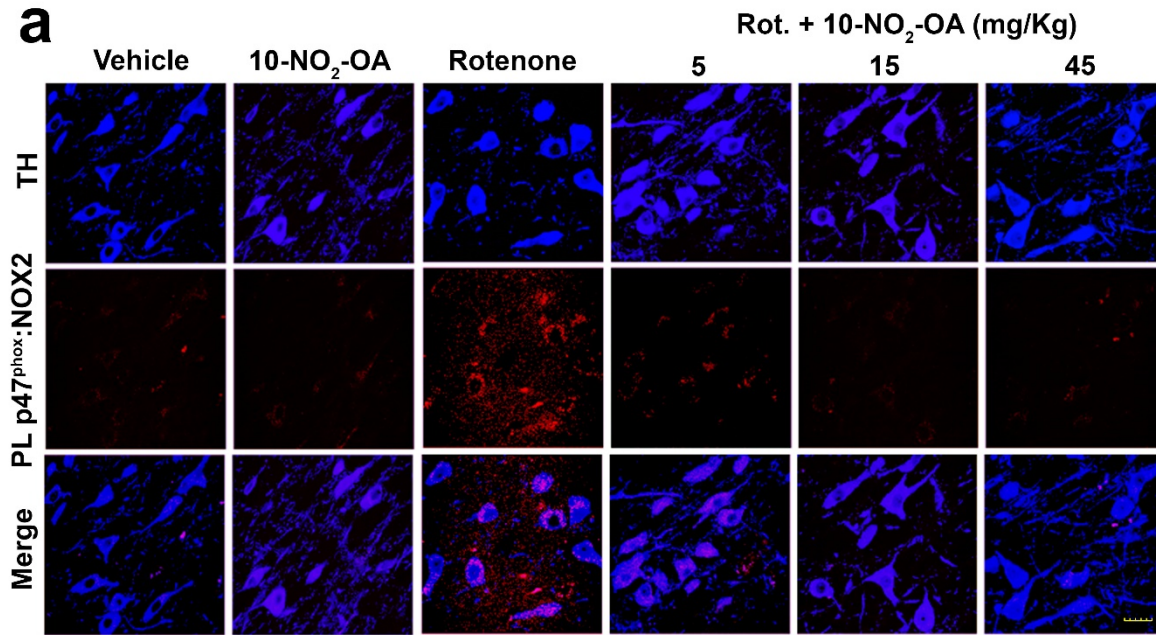
Supplementary Figure 4. Analysis of free 10-NO₂-OA and its inactive metabolite in rat brain (cohort 2). Brain concentrations of (a) 10-NO₂-OA, and (b) 10-NO₂-SA, five hours after the last treatments, were obtained by HPLC-MS/MS analysis using calibration curves in presence of the labeled internal standards 10-NO₂-[¹⁵N/D₄]OA and 10-NO₂-[¹⁵N/D₄]SA respectively. Representative extracted ion chromatograms in rat brain treated with Rotenone + 10-NO₂-OA, (c) the internal standard 10-NO₂-[¹⁵N/D₄]OA (upper panel, MRM 331.2/47) and 10-NO₂-OA (lower panel, MRM 326.2/46), and (d) the internal standard 10-NO₂-[¹⁵N/D₄]SA (upper panel, MRM 333.2/47) and 10-NO₂-SA (lower panel, MRM 328.2/46). nd = not detected.



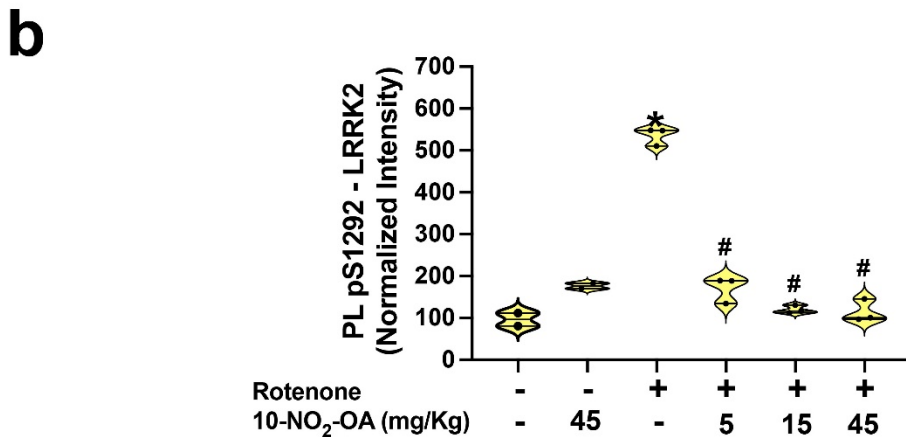
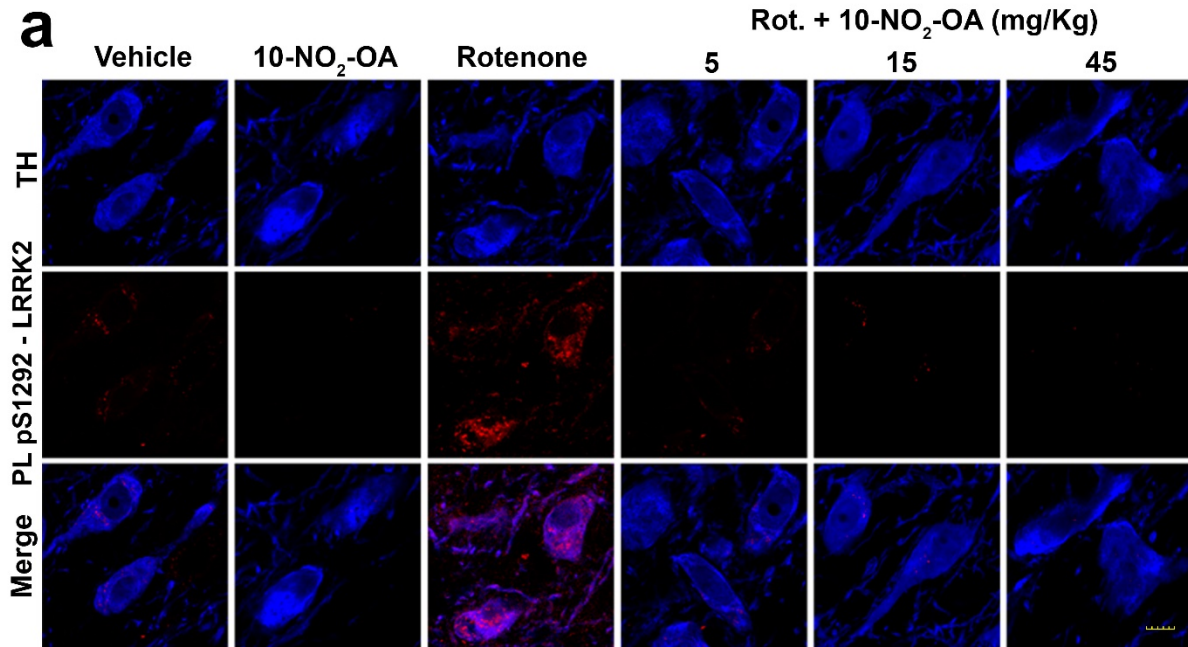
b



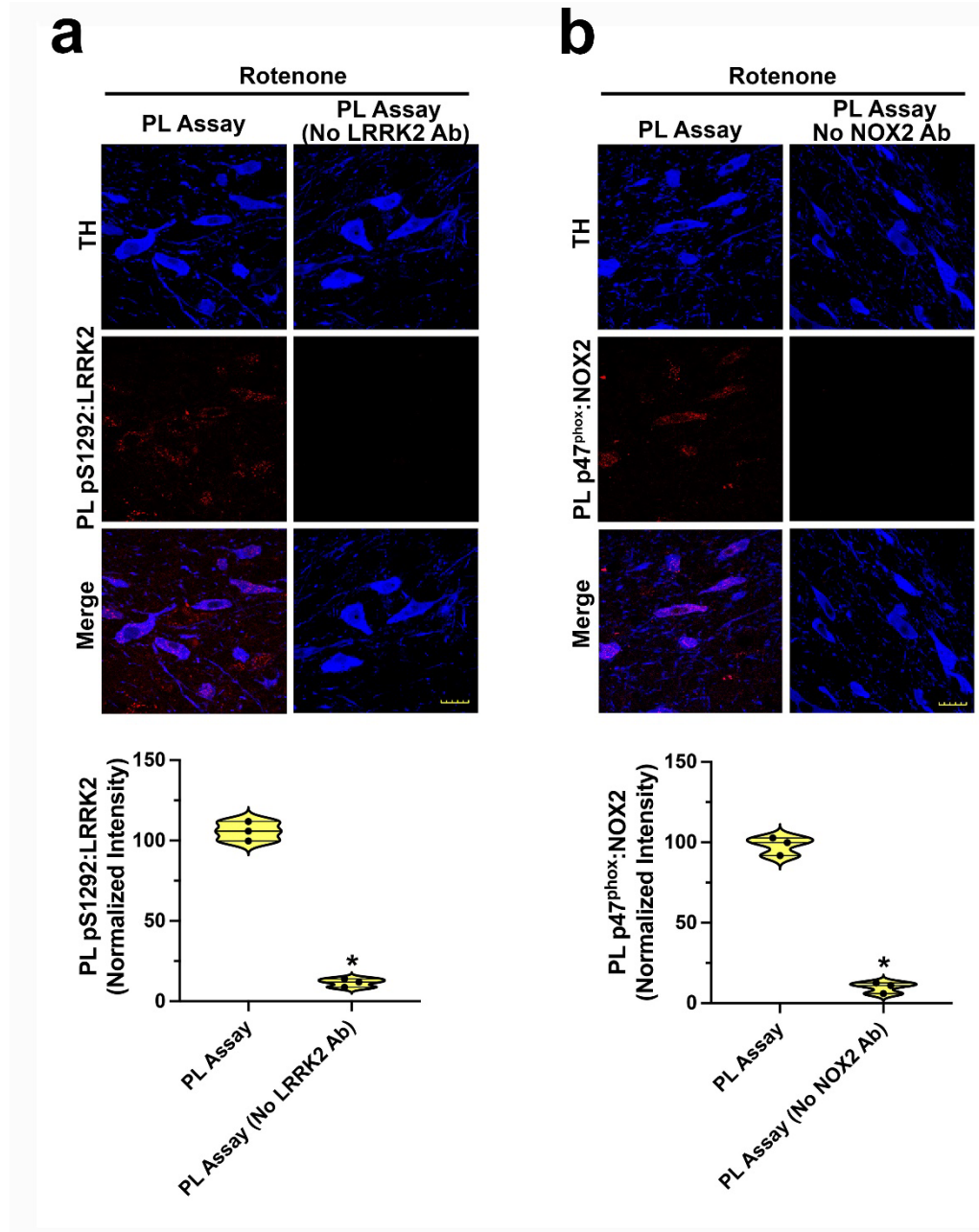
Supplementary Figure 5. 10-NO₂-OA inhibited lipid peroxidation (4-HNE) in the subacute PD model of rotenone. (a) 4-HNE immunostaining (red) in dopaminergic neurons (TH, blue) in the SNpc of rats (cohort 1 – Scale bar: 30μm) with below correspondent quantifications of the fluorescence signal (b). Symbols represent the normalized means of the intensity (with Vehicle set at 100%) from a single animal (6 slices/animal). Statistical analysis was performed by one-way ANOVA with post hoc Bonferroni correction (*, $p < 0.0001$ compared to Vehicle, #, $p < 0.0001$ compared to Rotenone).



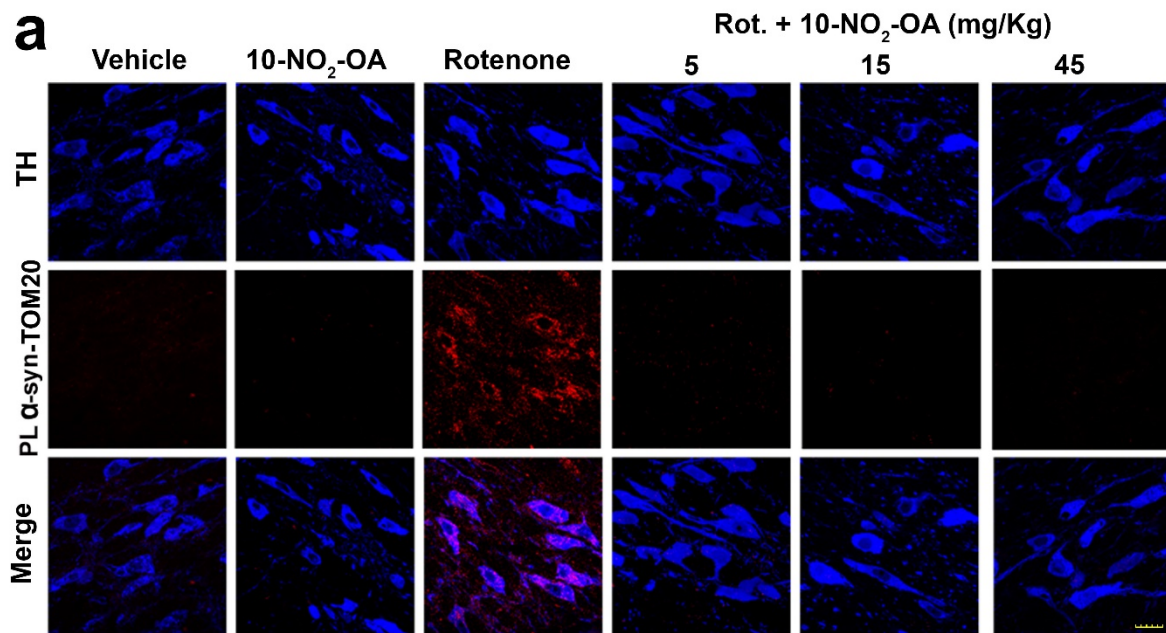
Supplementary Figure 6. 10-NO₂-OA inhibited NOX2 activation in SNpc of rat rotenone model. (a) PL p47^{phox}:NOX2 (red) in dopaminergic neurons (TH, blue) in the SNpc of cohort 1 rats (Scale bar: 30 μ m). (b) Quantifications of the fluorescence signal. Symbols represent the normalized means of the intensity (with Vehicle set at 100%) from a single animal (6 slices /animal). Statistical analysis was performed by one-way ANOVA with post hoc Bonferroni correction (*, $p < 0.0001$ compared to Vehicle, #, $p < 0.0001$ compared to Rotenone).



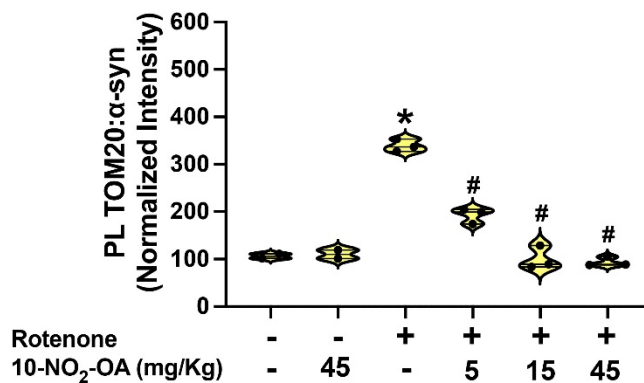
Supplementary Figure 7. 10-NO₂-OA prevented rotenone-induced LRRK2 activation in SNpc. (a) PL pS1292-LRRK2 (red) in dopaminergic neurons (TH, blue) in the SNpc of cohort 1 animals (Scale bar: 20 μ m). (b) Quantifications of the fluorescence signal. Symbols represent the normalized means of the intensity (with Vehicle set at 100%) from a single animal (6 slices /animal). Statistical analysis was performed by one-way ANOVA with post hoc Bonferroni correction (*, $p < 0.0001$ compared to Vehicle, #, $p < 0.0001$ compared to Rotenone).



Supplementary Figure 8. Validation of PL assays for LRRK2 and NOX2 by antibody depletion. (a, upper panel) PL pS1292:LRRK2 signal (red) disappears in dopaminergic neurons (TH, blue) not exposed to LRRK2 (N241A) Ab (Scale bar: 30 μ m). (a, lower graph) Quantification of the PL-related fluorescence signal. (b, upper panel) PL p47^{phox}:NOX2 signal (red) disappears in dopaminergic neurons (TH, blue) not exposed to NOX2 (gp91^{phox}) Ab (Scale bar: 30 μ m). (b, lower graph) Quantification of the PL-related fluorescence signal. Symbols represent the normalized means of the intensity (with rotenone set at 100%) from a single animal (6 slices/animal). Statistical analysis was performed by unpaired t-test (*, $p < 0.0001$).

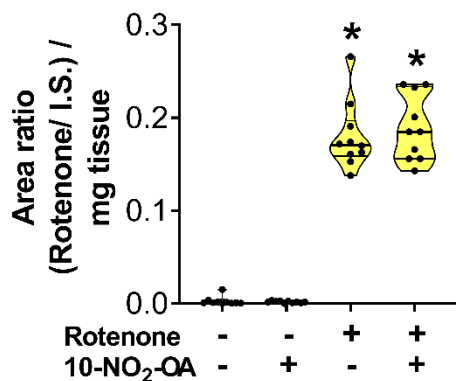


b



Supplementary Figure 9. 10-NO₂-OA inhibits α-synuclein-mediated mitochondrial import impairment in the subacute PD model of rotenone. (a) Confocal microscopy of PL α-synuclein:TOM20 (red) in dopaminergic neurons (TH, blue) in the SNpc of rats (cohort 1 - Scale bar: 30μm). (b) Quantification of the fluorescence signal. Symbols represent the normalized means of the intensity (with Vehicle set at 100%) from a single animal (6 slices /animal). Statistical analysis was performed by one-way ANOVA with post

hoc Bonferroni correction (*, $p < 0.0001$ compared to Vehicle, #, $p < 0.0001$ compared to Rotenone).



Supplementary Figure 10. Analysis of rotenone in whole rat brain (cohort 2). HPLC-MS-MS analysis of rotenone levels. Statistical analysis was performed by one-way ANOVA with post hoc Bonferroni correction (*, $p < 0.0001$ compared to Vehicle, and 10-NO₂-OA).